Available online at www.sciencedirect.com
SCIENCE DIRECT®
Journal of Molecular Spectroscopy 228 (2004) 580–592
Journal of MOLECULAR SPECTROSCOPY
www.elsevier.com/locate/jms

# Self- and $H_2$-broadened width and shift coefficients in the $2 \leftarrow 0$ band of $^{12}C^{16}O$: revisited

V. Malathy Devi,[a,*] A. Predoi-Cross,[b] D. Chris Benner,[a] M.A.H. Smith,[c] C.P. Rinsland,[c] and A.W. Mantz[d]

[a] *Department of Physics, The College of William and Mary, Box 8795, Williamsburg, VA 23187-8795, USA*
[b] *Department of Physics, The University of Lethbridge, 4401 University Drive, Lethbridge, AB, Canada*
[c] *Atmospheric Sciences, NASA Langley Research Center, MS 401A, Hampton, VA 23681-2199, USA*
[d] *Department of Physics, Astronomy and Geophysics, Connecticut College, 270 Mohegan Avenue, New London, CT 06320, USA*

Received 27 February 2004; in revised form 20 April 2004
Available online 7 June 2004

**Abstract**

Room temperature values for self-broadened and hydrogen-broadened Lorentz halfwidth coefficients, and self and hydrogen pressure-induced shift coefficients have been measured for transitions with rotational quantum number $m$ ranging between −24 and 24 in the $2 \leftarrow 0$ band of $^{12}C^{16}O$. The spectra were recorded with the McMath–Pierce Fourier transform spectrometer located at the National Solar Observatory on Kitt Peak. The analysis was performed using a multispectrum nonlinear least squares technique. We have compared our results with similar measurements published recently.
© 2004 Elsevier Inc. All rights reserved.

*Keywords:* CO; Self- and $H_2$-pressure broadening and shifts; Fourier transform infrared spectroscopy

## 1. Introduction

Given the increasing level of sophistication in remote sensing instrumentation, there is a need for accurate spectroscopic data relevant to planetary atmospheres such as Jupiter. Compared to the large number of papers published on line parameters in pure CO, there are relatively very few papers on measurements of broadening and shifting in CO perturbed by $H_2$. Any model or code for atmospheric absorption that requires linewidths measured to within 1–2% level of uncertainty, would require the shifts to be known to within 10% uncertainty. To achieve this level of accuracy for pressure shifts (that are typically 10 times smaller than the widths) the measurements have to be made using Fourier transform spectrometers or laser-based spectrometers. Even with these types of instrumentation, the reported error bars are often very large and there is disagreement between different data sets. One of the main objectives of the present spectroscopic study was to understand the differences between our previous measurements of $H_2$ broadened widths and shift coefficients [1] and those reported very recently by Sung and Varanasi [2]. The second objective was to check the overall reliability of our results by comparing our retrieved self-shifts and broadening parameters with other recent published results.

In the last five years there have been several experimental measurements of intensities, pressure broadening and pressure-induced shifts for transitions in the $2 \leftarrow 0$ band of $^{12}C^{16}O$ [1–5]. Some of these studies [2,4] involve the variation of the broadening and shift coefficients with temperature while other studies report line asymmetries caused by line mixing and various lineshape models [3,5]. In 2002 we reported measurements of self- and hydrogen broadening and shift coefficients in the $2 \leftarrow 0$ band of $^{12}C^{16}O$ from spectra recorded with the same instrument and analysis procedure [1] used in the present investigation. While the self-broadening and self-shift coefficients from [1] were in good agreement with other results reported in the literature, the

* Corresponding author. Fax: 1-757-864-7790.
*E-mail address:* m.d.venkataraman@larc.nasa.gov (V. Malathy Devi).

0022-2852/$ - see front matter © 2004 Elsevier Inc. All rights reserved.
doi:10.1016/j.jms.2004.05.006

Table 1
Summary of experimental conditions of the spectra

| | |
|---|---|
| Spectral coverage | 1850–5800 $cm^{-1}$ |
| Maximum path difference | 90.57–96.15 cm |
| Unapodized resolution (FWHM) | 0.0052–0.0055 $cm^{-1}$ |
| Number of co-added scans | 8–10 |
| Recording time | ~1 h |
| Signal-to-RMS noise | 200–500 |
| FTS input aperture size | 8 mm |
| Source | Glower at 125 V (self-broadened spectra) Oriel glowbar at 12 V ($H_2$-broadened spectra) |
| Beam splitter | KCl |
| Detectors | InSb |
| Optical filters | Wedged Ge/Quartz window |
| Self-broadened spectra | |
| Number of spectra | 6 |
| Absorbing pathlength | 10.0 cm |
| Pressure | ~3, 4.5, 9.5, 124, 280, and 507 Torr |
| Sample temperatures | 297 ± 1.0 K |
| $H_2$-broadened spectra | |
| Number of spectra | 5 |
| Absorbing pathlength | 150.0 cm |
| Total sample pressures | 94, 174, 332, 575, and 643 Torr |
| Sample temperatures | 296 ± 0.3 K |
| Volume mixing ratio of CO | ~5% |

760 Torr = 1 atm = 1013 hPa.

hydrogen-broadened halfwidth coefficients obtained from that study differed significantly from earlier studies [6–8], and the most recent measurements by Sung and Varanasi [2]. The reason for this large discrepancy is still puzzling to us and prompted us to record additional data and perform a new analysis.

## 2. Experimental details and data retrievals

The experimental procedure was basically the same as that described in [1]. The six self-broadened spectra used in the previous investigation [1] were included in the present analysis. For these six spectra the sample was contained at room temperature (~297 K) in a 10 cm glass cell with KCl windows. For the present study we recorded five new $H_2$-broadened spectra, also at room temperature (~296 K), utilizing a 1.5 m stainless steel absorption cell with KCl windows. The volume mixing ratios of CO in the CO–$H_2$ spectra were ~5%. The entire spectral region covering 4130–4340 $cm^{-1}$ was fit simultaneously in all 11 spectra. The summary of the experimental conditions is listed in Table 1.

A single self-broadened spectrum [1] and all the $H_2$-broadened CO spectra were acquired using a CO sample with 99.999 atom percent $^{12}C$ purchased from Matheson Gases. Five of the six self-broadened spectra were ob-

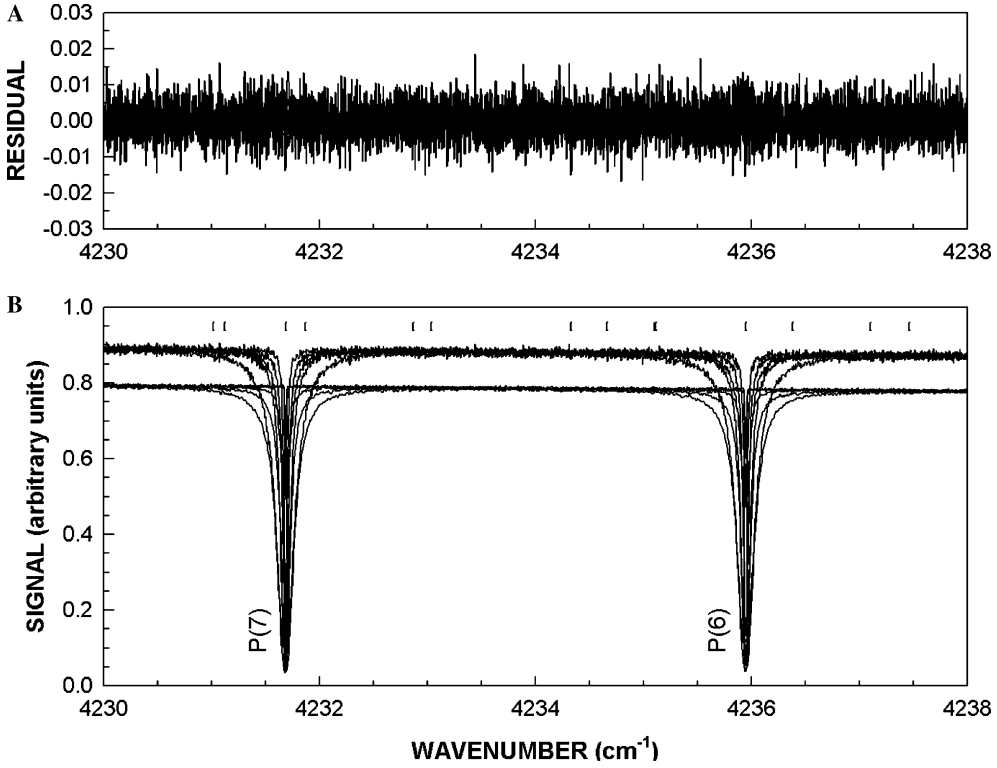


Fig. 1. A small segment (4230–4238 $cm^{-1}$) of the entire multispectrum fitted region from 4130 to 4340 $cm^{-1}$ of the $2 \leftarrow 0$ band of CO. Eleven observed spectra are shown in the lower panel (B), and the corresponding magnified residuals, observed minus calculated, appear in the upper panel (A). The six self-broadened spectra (lower background level) were recorded with a 10 cm cell, and the five $H_2$-broadened spectra (upper background level) were obtained with a 150 cm cell. The vertical tick marks shown in the bottom panel correspond to positions of spectral lines included in the multispectrum fit.

tained with a high-purity CO sample having natural isotopic composition (since $^{12}C^{16}O$ isotopomer constitutes ~98.7% of the sample, the error in spectral line intensity introduced due to small differences in the abundance of other isotopomers are negligible). The gas sample pressures and temperatures were monitored during the entire data acquisition period. At room temperature the rotational gas temperature agrees within 0.3 K or better with the thermocouple readings [9]. The gas pressures inside the cell (for the six self-broadened spectra) were measured and monitored with Datametrics Barocel 570A-series pressure transducers that were calibrated by the manufacturer to an absolute accuracy of 0.05% of the full-scale reading. The sample pressures of the five $H_2$-broadened CO spectra taken during the second experiment were measured and monitored using MKS Baratron gauges (1000 Torr pressure head) also calibrated to an absolute accuracy of 0.05% of full-scale

Table 2
Self- and $H_2$-broadened width and shift coefficients in the $2 \leftarrow 0$ Band of $^{12}C^{16}O$

| Line | $v$ ($cm^{-1}$)[a] | $b_L^0$(Self)[b] | $b_L^0(H_2)$[b] | $\delta^0$(Self)[b] | $\delta^0(H_2)$[b] |
|---|---|---|---|---|---|
| P (24) | 4148.796673 | 0.0477 (38) | 0.0696 (15) | −0.00712 (103) | |
| P (23) | 4154.211390 | 0.0512 (3) | 0.0683 (10) | −0.00728 (75) | −0.00694 (203) |
| P (22) | 4159.559472 | 0.0505 (2) | 0.0688 (7) | −0.00580 (53) | −0.00814 (15) |
| P (21) | 4164.840773 | 0.0520 (2) | 0.0680 (5) | −0.00593 (40) | −0.00732 (119) |
| P (20) | 4170.055146 | 0.0541 (1) | 0.0690 (4) | −0.00572 (30) | −0.00730 (68) |
| P (19) | 4175.202446 | 0.0558 (1) | 0.0692 (3) | −0.00558 (24) | −0.00648 (54) |
| P (18) | 4180.282526 | 0.0572 (1) | 0.0690 (3) | −0.00546 (20) | −0.00694 (44) |
| P (17) | 4185.295240 | 0.0576 (1) | 0.0689 (2) | −0.00505 (17) | −0.00636 (38) |
| P (16) | 4190.240441 | 0.0583 (1) | 0.0692 (2) | −0.00514 (15) | −0.00639 (34) |
| P (15) | 4195.117982 | 0.0589 (1) | 0.0686 (2) | −0.00533 (13) | −0.00597 (21) |
| P (14) | 4199.927718 | 0.0598 (1) | 0.0688 (2) | −0.00473 (12) | −0.00509 (19) |
| P (13) | 4204.669501 | 0.0616 (1) | 0.0695 (2) | −0.00455 (12) | −0.00560 (17) |
| P (12) | 4209.343184 | 0.0629 (1) | 0.0696 (2) | −0.00440 (12) | −0.00549 (17) |
| P (11) | 4213.948622 | 0.0640 (1) | 0.0699 (1) | −0.00454 (12) | −0.00539 (17) |
| P (10) | 4218.485666 | 0.0651 (1) | 0.0700 (1) | −0.00447 (11) | −0.00529 (16) |
| P (9) | 4222.954171 | 0.0656 (1) | 0.0699 (1) | −0.00459 (11) | −0.00516 (16) |
| P (8) | 4227.353988 | 0.0667 (1) | 0.0699 (1) | −0.00432 (11) | −0.00542 (16) |
| P (7) | 4231.684972 | 0.0683 (1) | 0.0698 (1) | −0.00415 (12) | −0.00542 (16) |
| P (6) | 4235.946976 | 0.0697 (1) | 0.0700 (1) | −0.00404 (12) | −0.00538 (16) |
| P (5) | 4240.139851 | 0.0724 (1) | 0.0699 (1) | −0.00400 (12) | −0.00545 (17) |
| P (4) | 4244.263453 | 0.0748 (1) | 0.0703 (1) | −0.00350 (13) | −0.00537 (18) |
| P (3) | 4248.317632 | 0.0771 (1) | 0.0703 (2) | −0.00324 (14) | −0.00551 (19) |
| P (2) | 4252.302244 | 0.0807 (1) | 0.0709 (2) | −0.00328 (17) | −0.00580 (22) |
| P (1) | 4256.217139 | 0.0873 (2) | 0.0761 (3) | −0.00309 (29) | −0.00534 (40) |
| R (0) | 4263.837197 | 0.0873 (2) | 0.0761 (2) | −0.00241 (26) | −0.00498 (36) |
| R (1) | 4267.542065 | 0.0807 (1) | 0.0709 (2) | −0.00273 (17) | −0.00503 (23) |
| R (2) | 4271.176630 | 0.0771 (1) | 0.0703 (2) | −0.00287 (14) | −0.00489 (20) |
| R (3) | 4274.740746 | 0.0748 (1) | 0.0703 (1) | −0.00320 (13) | −0.00495 (18) |
| R (4) | 4278.234264 | 0.0724 (1) | 0.0699 (1) | −0.00321 (13) | −0.00496 (18) |
| R (5) | 4281.657040 | 0.0697 (1) | 0.0700 (1) | −0.00356 (13) | −0.00500 (18) |
| R (6) | 4285.008925 | 0.0683 (1) | 0.0698 (1) | −0.00367 (12) | −0.00507 (18) |
| R (7) | 4288.289774 | 0.0667 (1) | 0.0699 (1) | −0.00383 (12) | −0.00518 (18) |
| R (8) | 4291.499439 | 0.0656 (1) | 0.0700 (1) | −0.00391 (13) | −0.00509 (18) |
| R (9) | 4294.637774 | 0.0651 (1) | 0.0700 (1) | −0.00391 (13) | −0.00486 (19) |
| R (10) | 4297.704633 | 0.0640 (1) | 0.0699 (1) | −0.00408 (13) | −0.00487 (19) |
| R (11) | 4300.699869 | 0.0629 (1) | 0.0696 (2) | −0.00443 (13) | −0.00520 (20) |
| R (12) | 4303.623335 | 0.0616 (1) | 0.0695 (2) | −0.00425 (14) | −0.00492 (20) |
| R (13) | 4306.474886 | 0.0598 (1) | 0.0688 (2) | −0.00427 (14) | −0.00551 (21) |
| R (14) | 4309.254375 | 0.0589 (1) | 0.0686 (2) | −0.00463 (15) | −0.00525 (23) |
| R (15) | 4311.961655 | 0.0583 (1) | 0.0692 (2) | −0.00466 (16) | −0.00503 (25) |
| R (16) | 4314.596582 | 0.0576 (1) | 0.0689 (2) | −0.00465 (18) | −0.00568 (29) |
| R (17) | 4317.159007 | 0.0572 (1) | 0.0690 (3) | −0.00492 (20) | −0.00534 (33) |
| R (18) | 4319.648786 | 0.0558 (1) | 0.0692 (3) | −0.00440 (23) | −0.00549 (40) |
| R (19) | 4322.065772 | 0.0541 (1) | 0.0690 (4) | −0.00570 (27) | −0.00578 (50) |
| R (20) | 4324.409820 | 0.0520 (2) | 0.0680 (5) | −0.00494 (34) | −0.00513 (64) |
| R (21) | 4326.680783 | 0.0505 (2) | 0.0688 (7) | −0.00591 (43) | −0.00441 (86) |
| R (22) | 4328.878516 | 0.0512 (3) | 0.0683 (10) | −0.00529 (59) | −0.00625 (118) |
| R (23) | 4331.002873 | 0.0477 (4) | 0.0696 (15) | | |

[a] The line center positions listed are from Pollock et al. [13].

[b] Halfwidth and pressure shift coefficients in units of $cm^{-1}\,atm^{-1}$ at 296 K. Values in parentheses are one-sigma uncertainties in the measured quantities in units of the last quoted digit.

reading. All the spectra were recorded at an unapodized resolution of 0.0052–0.0055 $cm^{-1}$.

The wavenumber scales of the CO–$H_2$ spectra were calibrated using the $v_3$ band lines of residual $^{12}C^{16}O_2$ [10,11] present in the evacuated spectrometer chamber as well as the nitrogen-purged atmospheric paths between the source and the entrance aperture of the spectrometer. For consistency, we also recalibrated the wavenumber scales of the self-broadened spectra relative to the positions of the $v_3$ $^{12}C^{16}O_2$ lines. This procedure was necessary since in the present CO–$H_2$ dataset, the residual water vapor transitions used in [1] were weak and deemed to be unreliable for calibration purposes.

The self-broadened widths, $H_2$-broadened widths, and pressure-induced shifts were determined by analyzing all eleven spectra simultaneously using an interactive multispectrum nonlinear least squares fitting technique [12]. The differences between the experimental spectra and the calculated spectra were minimized by treating the values of the various line parameters mentioned above as adjustable parameters in the least-squares solution. The absorption features were fitted using a Voigt lineshape profile. Judging from the flat pattern of the fit residuals (see Fig. 1), we did not consider that it was necessary to include line mixing or Dicke narrowing in our spectral profiles.

Initial values for the line positions, intensities and self-broadened widths were taken from the HITRAN database [10,11]. The HITRAN values for air-broadened widths and pressure-induced shifts were used as initial values for the $H_2$-broadened widths and shifts, and the self-shift coefficients had initial values of zero. The zero percent absorption background level for each spectrum was modeled using a fourth degree polynomial

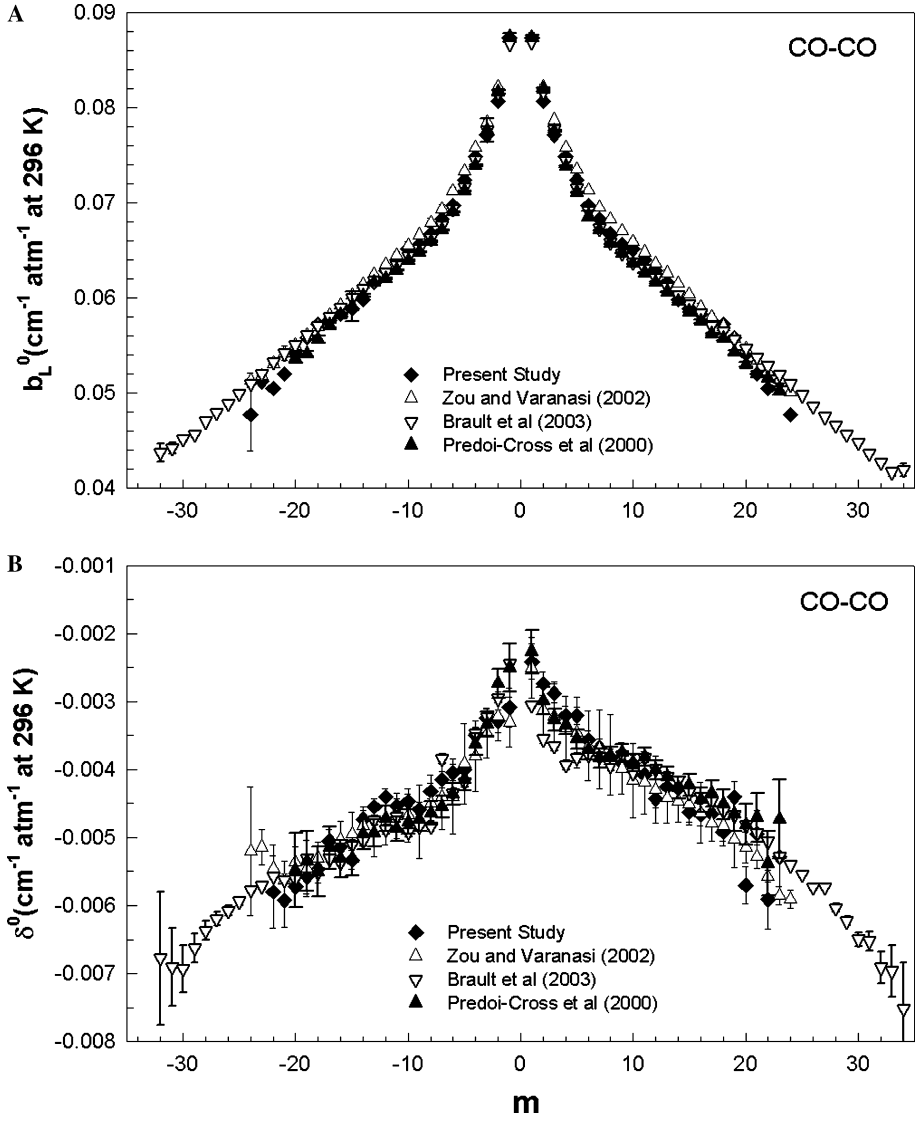


Fig. 2. (A) Measured $b_L^0$(self) versus $m$ ($m = -J''$ and $J'' + 1$ for the $P$ and $R$ branch lines, respectively). Present results are compared with other measurements published since 2000 [3–5]. Where error bars are not visible, the measurement uncertainties are smaller than the symbol size used. (B) The self-shift coefficients, $\delta^0$(self), determined in this work are compared to other values reported in the literature.

[12]. The multispectrum fits also accounted for the FTS phase error, FTS line shape for the McMath–Pierce FTS instrument, and the zero transmission level.

$$b_L(p,T) = p\left[b_L^0(\mathrm{H_2})(p_0,T_0)(1-\chi)\left[\frac{T_0}{T}\right]^{n1} + b_L^0(\mathrm{self})(p_0,T_0)\chi\left[\frac{T_0}{T}\right]^{n2}\right], \quad (1)$$

## 3. Analysis and results

The broadening and pressure-shift coefficients were retrieved using the following two equations:

$$v = v_0 + p\left[\delta^0(\mathrm{H_2})(1-\chi) + \delta^0(\mathrm{self})\chi\right]. \quad (2)$$

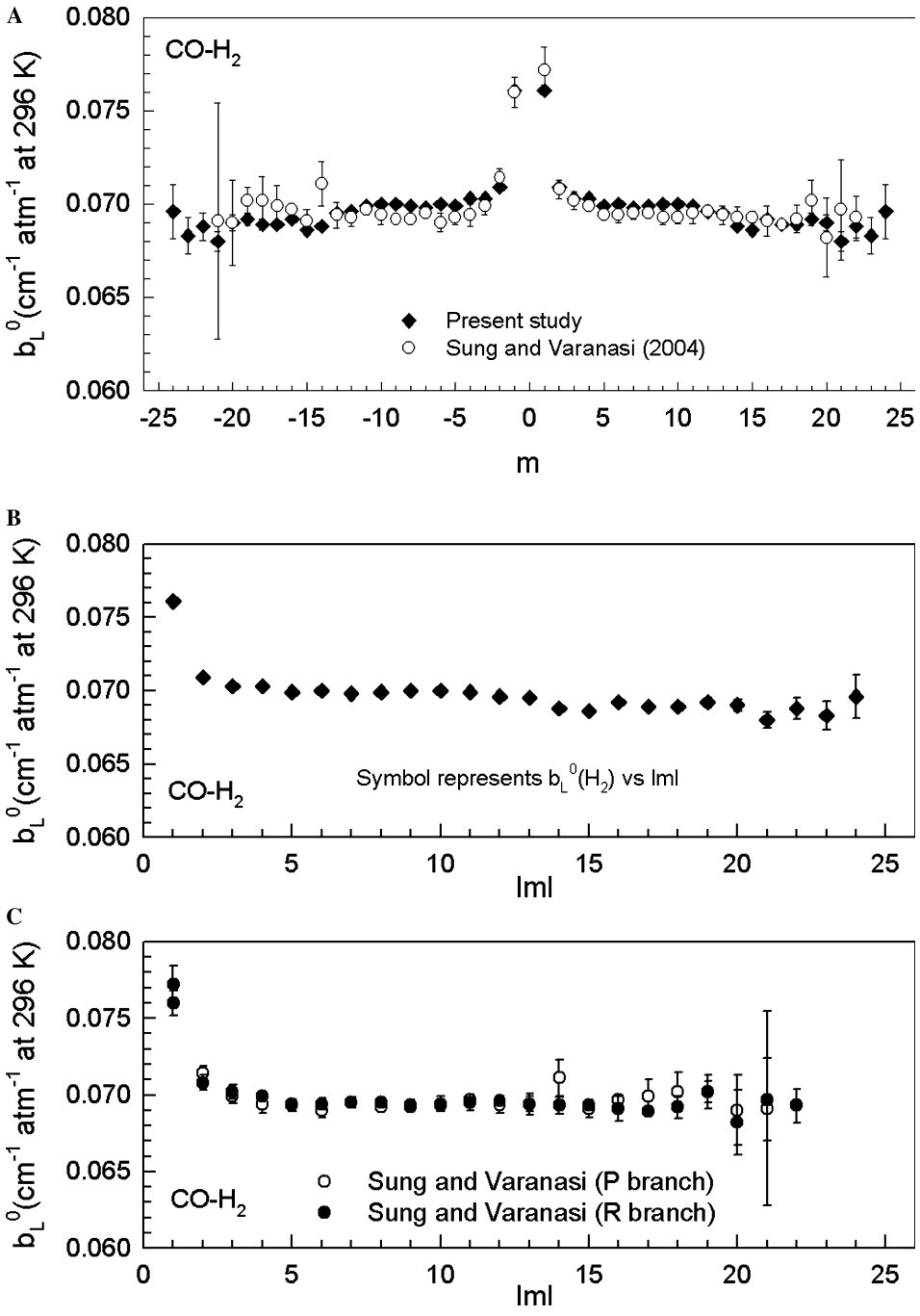


Fig. 3. (A) Measured $b_L^0(\mathrm{H_2})$ versus $m$ ($m = -J''$ and $J''+1$ for the $P$ and $R$ branch lines, respectively) in the $2 \leftarrow 0$ band of CO. Present results are compared with recent measurements published by Sung and Varanasi [2]. Where error bars are not visible, they are smaller than the symbol size used. The present measurements (B) and the measurements of Sung and Varanasi [2] (C) are re-plotted versus $|m|$ in the lower two panels.

In the above equations, $b_L^0$ and $\delta^0$ represent pressure broadening and pressure shift coefficients (in $cm^{-1}$ $atm^{-1}$ at 296 K), respectively. $b_L(p,T)$ is the Lorentz halfwidth (in $cm^{-1}$) of the spectral line at pressure $p$ and temperature $T$, and $b_L^0(\mathrm{Gas})(p_0,T_0)$ is the Lorentz halfwidth of the line at the reference pressure $p_0$ (1 atm) and temperature $T_0$ (296 K) of the broadening gas (either $H_2$ or CO), and $\chi$ is the ratio of the partial pressure of CO to the total sample pressure in the cell. The temperature dependence exponents of the pressure-broadening coefficients are given by $n1$ and $n2$. In our study the temperature corrections were small because $T$ (296–298 K) was close to $T_0$ (296 K). For the temperature dependences of both the $H_2$-broadening and self-broadening coefficients we assumed a value of 0.69 for each line which is the constant value for temperature-dependence of air-broadening given in the HITRAN database [10,11]. This value is close (within ~10%) to the temperature-dependence exponents experimentally determined by Sung and Varanasi [2] and Varanasi et al. [6] for $H_2$-broadening in the $1 \leftarrow 0$ band and by Zou and Varanasi [4] for self-broadening in the $2 \leftarrow 0$ band of $^{12}C^{16}O$. Since the gas sample temperatures in our data were close to 296 K, assuming this constant $n$ value for both self- and $H_2$-broadening did not introduce any error larger than 0.006% in the retrieved broadening coefficients. In Eq. (2), $v_0$ is the zero-pressure line position (in $cm^{-1}$), and $v$ is the line position corresponding to the pressure $p$. In our analysis the temperature dependences for all self-shift and $H_2$-shift coefficients were set to a fixed value of zero. This assumption also did not introduce any noticeable residuals in the least squares fits.

All lines were assumed to have a Voigt lineshape convolved with the instrument lineshape function appropriate to the McMath–Pierce FTS. As mentioned in the previous section, the Voigt lineshape was found adequate to fit all our data to within the noise level of the spectra. This is illustrated in Fig. 1, where we show a relatively small segment (4230–4238 $cm^{-1}$) of the entire multispectrum fitted interval. Details about the analysis procedure and error estimates are given in [1].

There is one important difference between the present analysis and our previous study [1]. Previous broadening studies by various investigators [1–8] have shown that within experimental uncertainties the broadening coefficients are symmetric in the $P$ and $R$ branches. That is, lines with identical $|m|$ values in the $P$ and $R$ branches will have the same halfwidth coefficients ($m = -J''$ in the $P$ branch and $J''+1$ in the $R$ branch). Our multispectrum analysis procedure [12] has been modified to include the capability to introduce constraints on certain retrieved spectroscopic parameters. In the present work, for both self- and $H_2$-broadening, we have constrained the $P$ and $R$ branch halfwidth coefficients to be the same for each $|m|$ value. These constraints were implemented interactively during the multispectrum fitting process. Introducing this constraint into the solution reduced the uncertainty normally change in the broadening coefficients with identical $|m|$ values in the $P$ and $R$ branches that arise due to sources such as signal-to-RMS noise in the data and presence of neighboring lines.

The results from the present analysis are listed in Table 2. The uncertainties listed in parentheses are one standard deviation of the measured quantities in units of the last quoted digits due only to the noise levels of the spectra. The absolute uncertainty in the measured broadening coefficients is estimated to be ~2% plus the uncertainty listed in Table 2. Based upon the same uncertainty considerations as those for broadening coefficients, we estimate the absolute uncertainty in shift coefficients to be about 10% in addition to the uncertainty listed in Table 2. For the majority of the CO lines

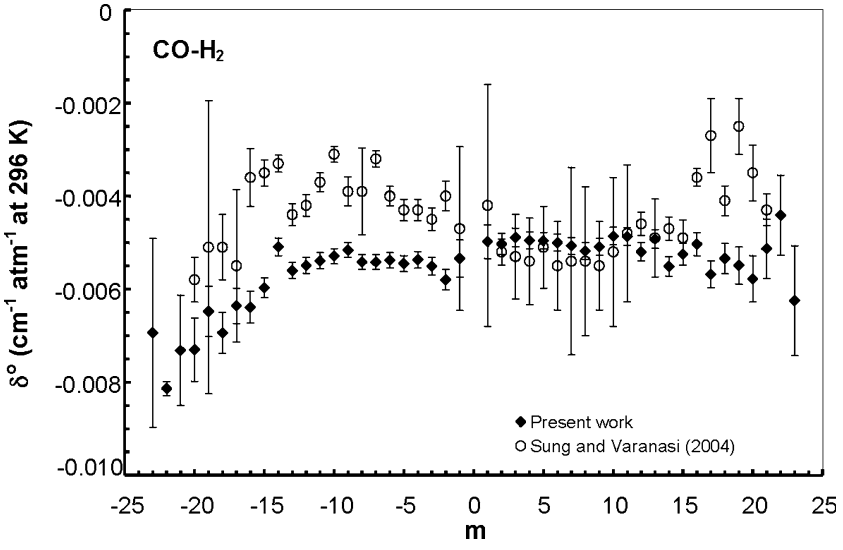


Fig. 4. Measured hydrogen pressure shift coefficients $\delta^0(H_2)$ in the $2 \leftarrow 0$ band of CO. Values from the present work are plotted as a function of $m$ along with the results from Sung and Varanasi [2].

the precision in our measured line center positions was $0.00003\,cm^{-1}$. However, the line positions from Pollock et al. [13] are listed in Table 2 because of the higher absolute accuracy of [13] compared to that obtained in the present study. Because the intensity and self-broadening are correlated we compared the retrieved intensities with those reported in [1] and found that the two sets of intensities agree within 0.04%. Intensities obtained from present measurements agree within a percent with values reported by Sung and Varansi [2]. Constraining the broadening coefficient for $P$ and $R$ branch transitions with the same $|m|$ value reduces the uncertainties of the retrieved intensities.

The measured self-broadening coefficients, $b_L^0$(self) versus $m$ ($m = -J''$ and $J'' + 1$ for the $P$ and $R$ lines, respectively) are plotted in Fig. 2. In the upper panel (A), we have compared the present results with other recent measurements [3–5]. Because of the much larger optical densities used in their experiment, the authors of [5], were able to measure both the broadening and shift coefficients to much higher $m$ values than the present work. In the lower panel (B) we have compared the self-shift coefficients with values reported in [3–5].

The present $H_2$-broadening coefficients are compared with the recent measurements by Sung and Varanasi [2] and shown in Fig. 3. In panels (B) and (C) we have plotted the $H_2$ broadening coefficients as a function of $|m|$ determined in the present work and in [2], respectively. Comparisons of previous CO–$H_2$ broadening

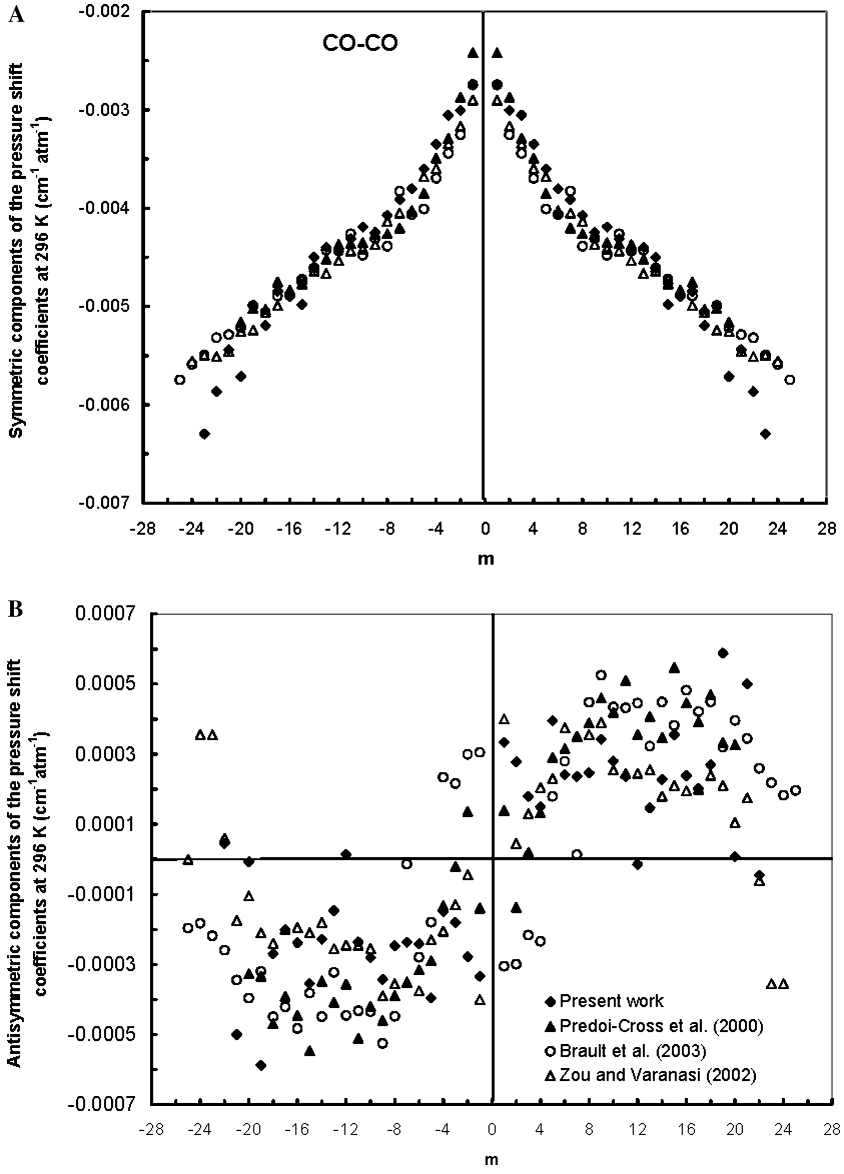


Fig. 5. The symmetric (A) and antisymmetric (B) components of self-induced shifts in the $2 \leftarrow 0$ band of $^{12}C^{16}O$. Previous measurement results [3–5] are included for comparison.

results with other similar measurements have been shown in [1], and therefore will not be repeated here. Because of the constraints used in the present work, the width coefficients in the $P$ and $R$ branches are indistinguishable in panel (B), small differences in values between the two branches are obvious in panel (C). Our multispectrum analysis technique with constraints included in the solution is the best way to extract all of the information from the spectra. First, no systematic residuals were present in the fit. Second, since no systematic residuals were present in the fit, removal of the constraints would only add additional free parameters to the solution, and this can only result in overfitting of the data. The validity of the constraints to the level of our uncertainties Table 2 has been proven by the fact that there are no remaining systematic residuals. Least squares solution with more free (unconstrained) parameters cannot legitimately extract more information. The $H_2$ pressure induced shifts determined from this work are displayed in Fig. 4 along with those obtained by Sung and Varanasi [2]. The shift coefficients compare well in the $R$ branch while the shift coefficients in the $P$ branch are somewhat different in the two studies.

The pressure-induced shift coefficient $\delta_0$ may be decomposed as a function of $m$ into two components: a isotropic (angle independent) component, $\delta_{0-s}(m) = [\delta^0(m) + \delta^0(-m)]/2 = [\delta^{0-R}(J+1) + \delta^{0-P}(J)]/2$, and an anisotropic component, $\delta_{0-a}(m) = [\delta^0(m) - \delta^0(-m)]/2 = [\delta^{0-R}(J+1) - \delta^{0-P}(J)]/2$. Neglecting the rotation–vibration interaction, the vibrational dephasing contribu-

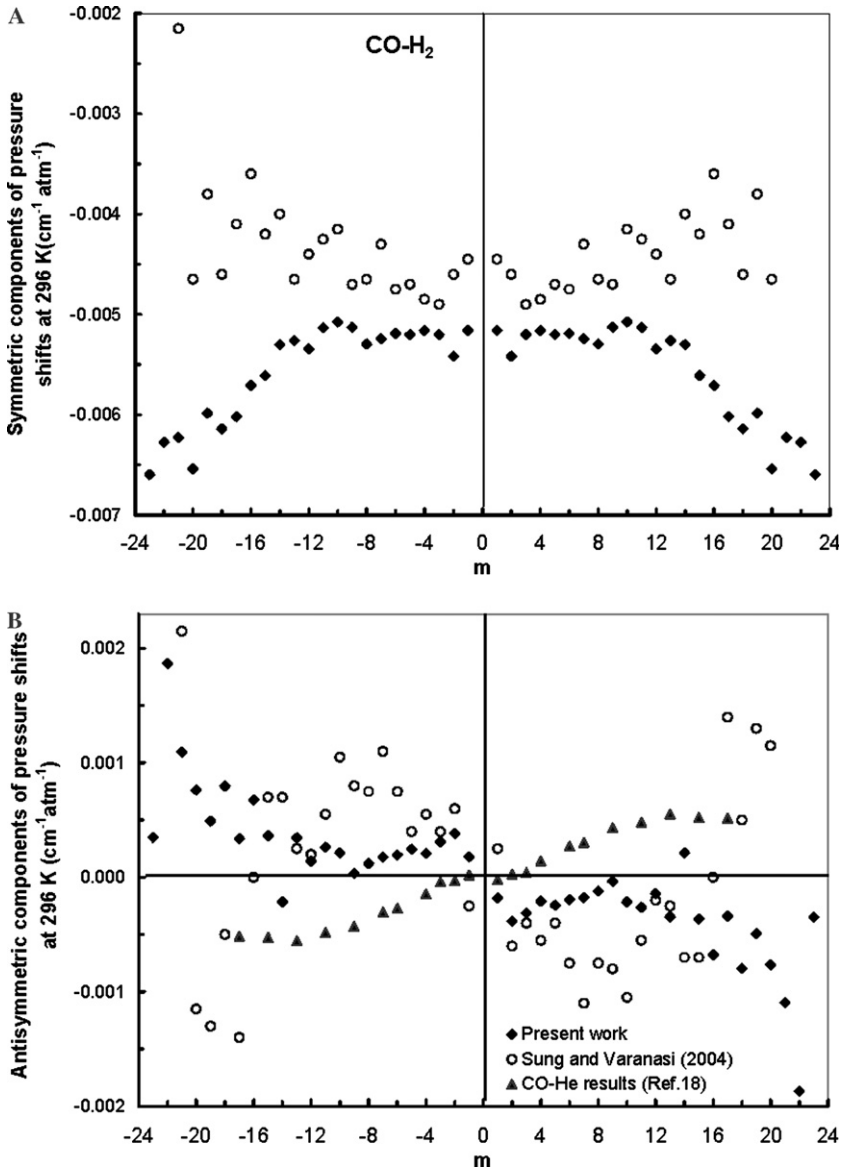


Fig. 6. The symmetric (A) and antisymmetric (B) components of hydrogen-induced line shifts in the $2 \leftarrow 0$ band of $^{12}C^{16}O$. Also included are the results of Sung and Varanasi [2].

tion coming from the isotropic part of the potential is symmetric in the $P$ and $R$ branches, such that $\delta_{0-s}(m) = \delta_{0-s}(-m)$.

The isotropic long-range potential tends to decrease with the vibrational frequency while the isotropic short-range potential has the opposite effect [14,15]. As expected, the balance between the two is temperature dependent. In Raman spectra of gaseous $H_2$, the shift changes sign with temperature [16].

The symmetric and antisymmetric parts of the pressure-induced shift coefficients for CO–CO and CO–$H_2$ are plotted in Figs. 5 and 6, respectively. Except for very low $|m|$ and $|m| > 20$, our results for CO–CO are in good agreement with previous measurements [4]. The symmetric components of the shifts reported in [2] for CO–$H_2$ show somewhat larger scatter with a pattern very different than the one obtained from the present data set. There are no known theoretical calculations of the CO–$H_2$ shifts for this band with which comparisons of present results could be made.

As shown in Fig. 6 our values for $\delta_{0-s}(m)$ are nearly constant, and thus may be interpreted as a shift of the band as a whole, i.e., as a shift in the vibrational frequency. Based upon our experimental data, it appears that for CO–$H_2$ that the long range (the $R^{-6}$ dependent) term of the potential dominates the shift at room temperature. Following the approach from [16], an accurate investigation would require experimental shift data recorded at least at two temperatures and a knowledge of the short-range potential.

The antisymmetric component, $\delta_{0-a}(m)$, arises from the anisotropic part of the interaction potential and is antisymmetric in the line number $m$, such that $\delta_{0-a}(m) = -\delta_{0-a}(-m)$. The observed pattern of $\delta_{0-a}(m)$ for CO–CO (see Fig. 5B) approximately follows a straight line through the origin, suggesting that the band is either stretched or compressed as a whole due to a change in the value of the rotational constant. If, as suggested above, the long-range (the $R^{-6}$ dependent) term of the potential dominates the shift at room temperature, the molecule is stretched so it oscillates in a softer part of the vibrational well. As a consequence, the rotational constant $B$ decreases. This argument is consistent with the pattern seen in Fig. 5B for $\delta_{0-a}(m)$ of CO–CO.

The term $\delta_{0-a}(m)$ is dominated by anisotropic forces [17]. For CO–$H_2$, the major part of the anisotropic potential comes from the isotropic part of $H_2$ and the anisotropic part of CO. The separation of nuclei in $H_2$ is very small and one would expect that the pattern of $\delta_{0-a}(m)$ presented in Fig. 6B to be similar with the one observed for CO–He [18]. However, the slopes of the two observed patterns are opposite.

Herman [17] had established a number of theoretical rules for widths and shifts, based on the Anderson–Tsao–Curnutte (ATC) theory [19,20]. One of them involves the "Herman" factor (constant), $H$:.3

$$H = [\delta^0(m) + \delta^0(-m)][b_L^0(m) + b_L^0(-m)]^{\frac{3}{2}}, \tag{3}$$

where $\delta^0$ and $b_L^0$ are the pressure shifting and Lorentz broadening coefficients, respectively. This rule based on semi-classical theory states that $H$ is independent of $m$. In Fig. 7 we have plotted the $H$ factor for pure CO and CO–$H_2$ mixtures, using our measurement results. The experimental value of $H$ is nearly constant, except for very low $|m|$ and $|m|$ values above 20. We acknowledge that modern theoretical treatments may prove that the $H$ factor is not completely independent of $m$. However, the pattern of our experimental values of $H$ suggests that the semi-classical approximation is reasonable and

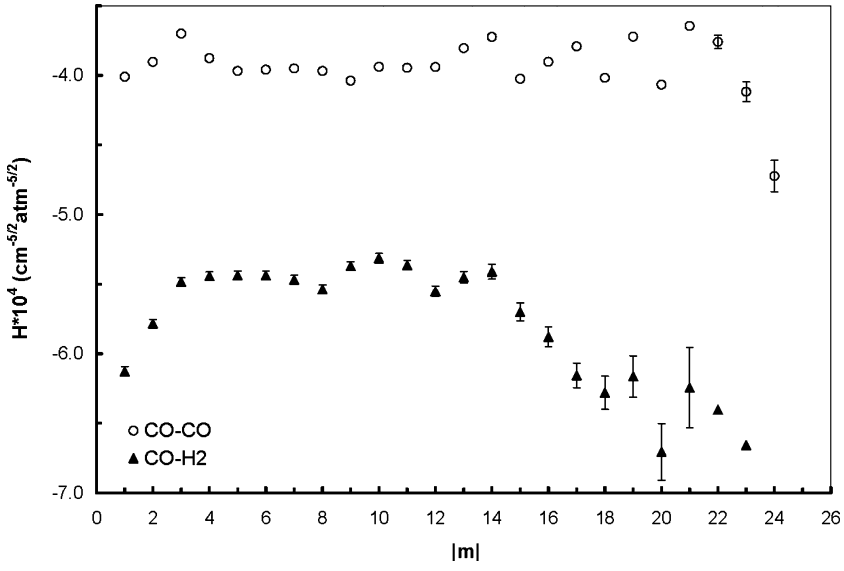


Fig. 7. The Herman factor plotted as a function of $|m|$ for the present CO–CO and CO–$H_2$ results.

Table 3
Coefficients of a power-law polynomial in $\ln|m|$ for the Lorentz broadening coefficients of pure CO and CO–$H_2$ at 296 K

| Coefficient | CO–CO | CO–$H_2$ |
|---|---|---|
| $b_L^0$ ($cm^{-1}$ $atm^{-1}$) | 87.31935 (27) | 76.09439 (36) |
| $a_0$ | −0.2583742 (62) | −0.17651 (45) |
| $a_1$ | +0.397765 (58) | +0.13854 (71) |
| $a_2$ | −0.36584 (72) | −0.04611 (68) |
| $a_3$ | +0.137011 (89) | +0.00526 (47) |
| $a_4$ | −0.01855 (69) | −0.00001 (56) |

ultimately increases our confidence in the reliability of our shift and Lorentz broadening results.

As shown in [21] we have fitted the CO–CO and CO–$H_2$ broadening coefficients with smooth functions of $|m|$ having the form:

$$b_L^0(m) = b^0|m|^a, \tag{4}$$

where $a$ is given by $a_0 + a_1(\ln|m|) + a_2(\ln|m|)^2 + a_3(\ln|m|)^3 + a_4(\ln|m|)^4$. The fitted values of the coefficients are given in Table 3. The coefficients can be used to calculate the broadening coefficients with an estimated uncertainty of ±0.3%, within the range of $|m|$ values reported in Table 2. Plots of the experimental and fitted broadening coefficients for pure CO and CO–$H_2$ at 296 K are presented in Figs. 8 and 9, respectively. The plots of $b_L^0(m)_{obs} - b_L^0(m)_{fit}$ do not show a completely random scatter in the residuals. For the case of CO–CO and CO–$H_2$ broadenings the residuals are within the three sigma uncertainties of the measurements (Table 2, Figs. 8 and 9), and we feel it is not useful to add additional terms to improve the fit at this time.

The self-broadening coefficients have also been fitted using two other empirical expressions, namely a cubic expression and the expression used by Sung and Varanasi [22] in their study of the $3 \leftarrow 0$ band of CO. The cubic polynomial is given by:

$$b_L^0 = c_0 + c_1|m| + c_2|m|^2 + c_3|m|^3 \tag{5}$$

and the expression used by Sung and Varanasi [22] is written as:

$$b_L^0 = \frac{(b + c|m|)}{N + |m|}. \tag{6}$$

In Eqs. (5) and (6) $c_0$–$c_3$, $b$ and $c$ are the coefficients of the fit and $N$ is an integer. Several values of $N$ were used and the best fit is obtained with $N = 12$. We found that using a fourth (or higher) degree polynomial in $|m|$ to fit the self-broadened coefficients resulted in a worse fit than a third degree polynomial given by Eq. (5).

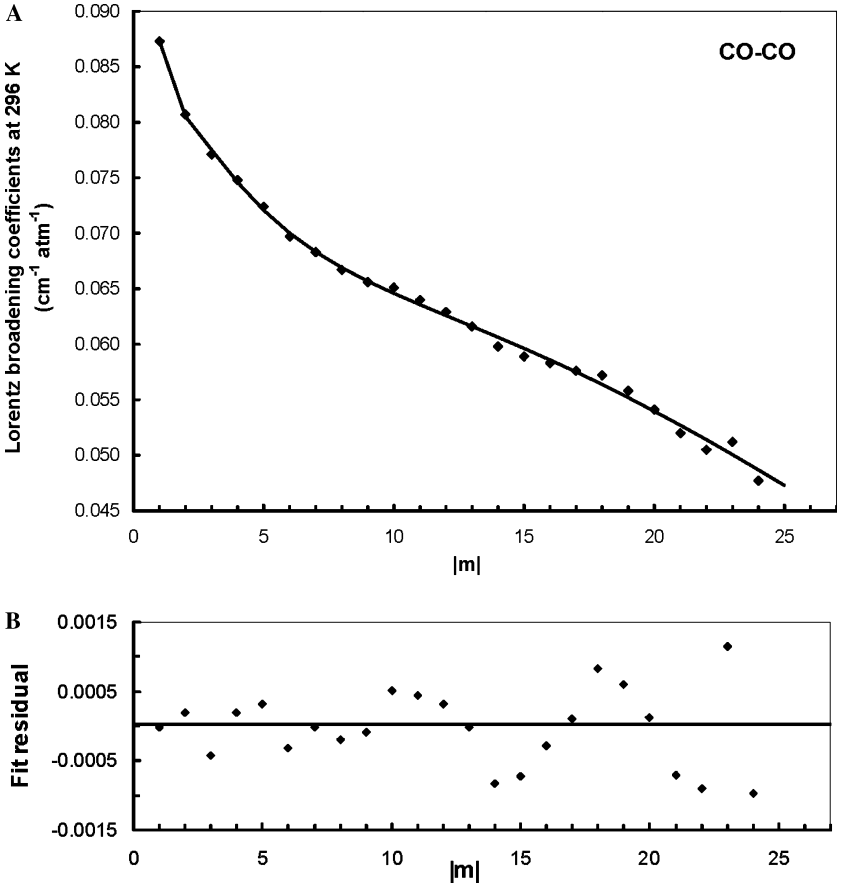


Fig. 8. (A) CO $2 \leftarrow 0$ self-broadening coefficients, $b_L^0$(self), plotted as a function of $|m|$. The solid continuous curve is the best fit of Eq. (4) to the present measurements (symbols). (B) The residual differences between the experimental values and the fitted curve.

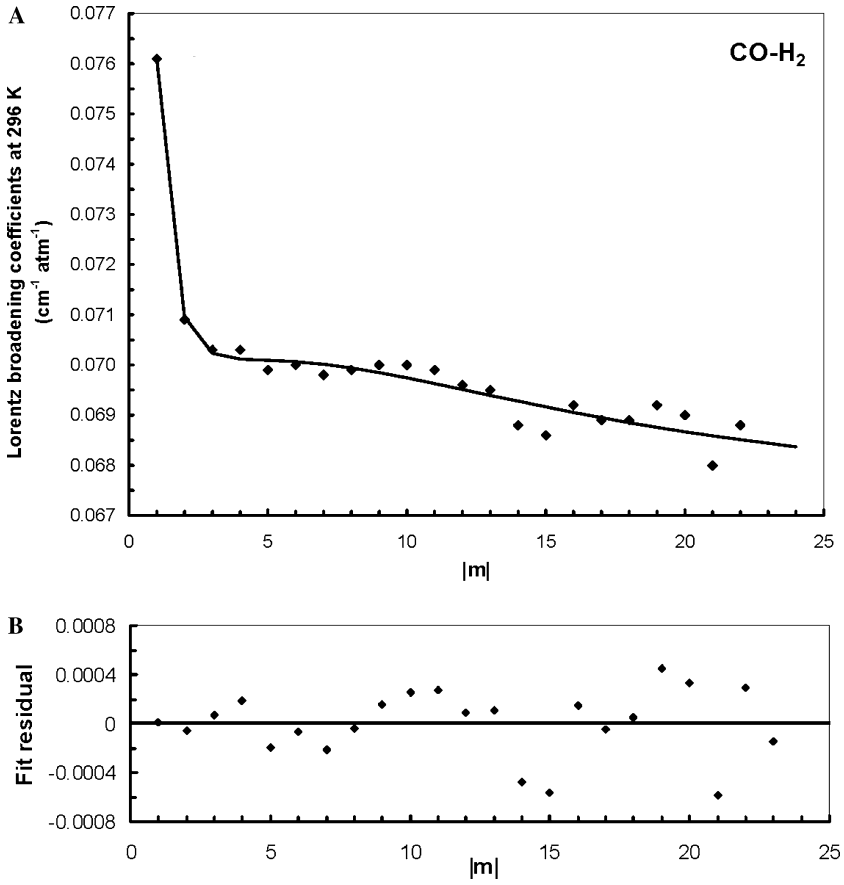


Fig. 9. Same as Fig. 8, but for CO $2 \leftarrow 0$ $H_2$-broadening coefficients, $b_L^0(H_2)$.

Table 4
The coefficients obtained by fitting Eqs. (5) and (6) to the present measurements of self-broadened widths in the CO $2 \leftarrow 0$ band

| Coefficients | Third degree polynomial | Coefficients | Sung and Varanasi formula [22] |
|---|---|---|---|
| $c_0$ | $(8.968 \pm 0.063) \times 10^{-2}$ | $b$ | $1.0954 \pm 0.0082$ |
| | $8.938 \times 10^{-2}$ | | 1.086 |
| $c_1$ | $-(4.006 \pm 0.21) \times 10^{-3}$ | $c$ | $(3.324 \pm 0.078) \times 10^{-2}$ |
| | $-4.013 \times 10^{-3}$ | | 0.0347 |
| $c_2$ | $(2.004 \pm 0.20) \times 10^{-4}$ | $N$ | 12 |
| | $2.089 \times 10^{-4}$ | | 12 |
| $c_3$ | $-(4.315 \pm 0.51) \times 10^{-6}$ | | |
| | $-4.654 \times 10^{-6}$ | | |

The values listed on the second line for each coefficient are from Sung and Varanasi [22] for self-broadening in the $3 \leftarrow 0$ band of CO.

The coefficients obtained using expressions (5) and (6) are given in Table 4 along with the values for $3 \leftarrow 0$ band from [22]. As shown in [22] and plotted in Fig. 10, the fitted curve using the cubic polynomial expression deviates very quickly from measurements if extended beyond the measured range of $m$ and the curve using the formula of Sung and Varanasi [22] follows the measured values and shows a smooth extrapolation of broadening coefficients to much higher values of $m$. The coefficients we obtained by fitting our $2 \leftarrow 0$ band self-broadened halfwidths to Eq. (6) agree quite well with values published by Sung and Varanasi [22] for the $3 \leftarrow 0$ band. We were not able to fit successfully the $H_2$-broadened width coefficients using either the third degree polynomial or the formula developed by Sung and Varanasi [22].

## 4. Conclusions

We have recorded new hydrogen-broadened CO spectra and measured the hydrogen broadening and hydrogen pressure induced shift coefficients in the $2 \leftarrow 0$ band of $^{12}C^{16}O$ in order to clarify the disparity between our previous results published a year ago with other recent measurements. Our multispectrum nonlinear least squares fitting technique has been modified and we have

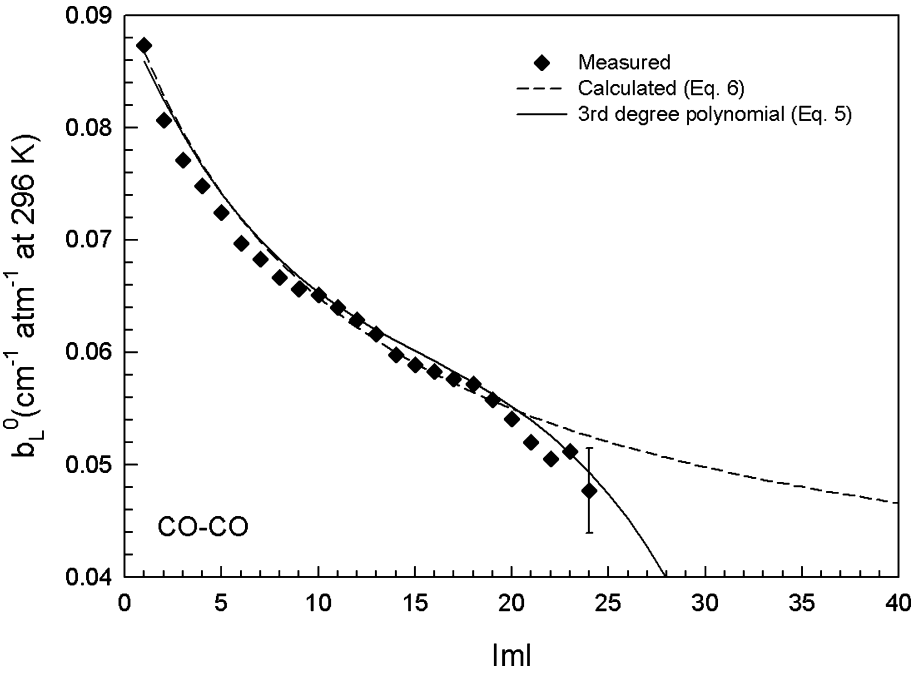


Fig. 10. Other empirical representations of the room temperature CO self-broadening coefficients in the $2 \leftarrow 0$ band (symbols). Solid curve is for a third-degree polynomial (Eq. (5)), and the dashed curve represents the best fit of the measurements to the Sung and Varanasi [22] expression (Eq. (6)). Constants are given in Table 4.

added certain constraints in the fitted parameters. We were able to fit all the spectra simultaneously to the noise level assuming the rotational dependence of the hydrogen-broadened (and self-broadened) width was the same in the $P$ and $R$ branches. Although speed-dependent lineshape profile and asymmetry line parameters were incorporated by other investigators in the analysis of $2 \leftarrow 0$ and $3 \leftarrow 0$ bands of CO, we were able to fit our data to the noise level of the spectra with a Voigt lineshape.

The present $H_2$-broadening measurements agree well with the recent study by Sung and Varanasi [2], but there is some disagreement among the hydrogen pressure-shift coefficients between these two studies. Since the self-broadened CO spectra were also included in the multi-spectrum fits, self-broadening and self-shift coefficients were determined simultaneously with the corresponding $H_2$ broadening and shift parameters. The self-broadening and self-shift coefficients agree well with our previous measurements [1] and with those reported by Predoi-Cross et al. [3], Zou and Varanasi [4] and Brault et al. [5]. We were able to model the $|m|$-dependence of both the self- and $H_2$-broadening coefficients within 1% uncertainty using a power-law polynomial of the same form as in [21].

## Acknowledgments

The authors thank Mike Dulick and Detrick Branston of the National Solar Observatory (NSO) for their assistance in obtaining the data. Sincere thanks go to Professor A. David May for reading the manuscript and making many useful suggestions. Arlan W. Mantz acknowledges partial support through a NASA EPSCOR grant, NCC5-601, as well as the Sherman Fairchild Foundation. Cooperative agreements and contracts with National Aeronautics and Space Administration supported the research at the College of William and Mary. The Association of Universities for Research in Astronomy, operates NSO under contract with the National Science Foundation. A. Predoi-Cross has been supported by a University of Lethbridge start up research fund.

## References

[1] V. Malathy Devi, D. Chris Benner, M.A.H. Smith, C.P. Rinsland, A.W. Mantz, J. Quant. Spectrosc. Radiat. Transfer 75 (2002) 455–471.
[2] K. Sung, P. Varanasi, J. Quant. Spectrosc. Radiat. Transfer 85 (2) (2004) 165–182.
[3] A. Predoi-Cross, J.P. Bouanich, D. Chris Benner, A.D. May, J.R. Drummond, J. Chem. Phys. 113 (2000) 158–168.
[4] Q. Zou, P. Varanasi, J. Quant. Spectrosc. Radiat. Transfer 75 (2002) 63–92.
[5] J.W. Brault, L.R. Brown, C. Chackerian Jr., R. Freedman, A. Predoi-Cross, A.S. Pine, J. Mol. Spectrosc. 222 (2003) 220–239.
[6] P. Varanasi, S. Chudamani, S. Kapur, J. Quant. Spectrosc. Radiat. Transfer 38 (1987) 167–171.
[7] J.-P. Bouanich, C. Brodbeck, J. Quant. Spectrosc. Radiat. Transfer 13 (1973) 1–7.

[8] M.F. Le Moal, F. Severin, J. Quant. Spectrosc. Radiat. Transfer 35 (1986) 145–152.
[9] A. Predoi-Cross, C. Hnatovsky, K. Strong, J.R. Drummond, D. Chris Benner, J. Mol. Struct. 695–696 (2004) 269–286.
[10] L.S. Rothman, C.P. Rinsland, A. Goldman, S.T. Massie, D.P. Edwards, J.-M. Flaud, A. Perrin, C. Camy-Peyret, V. Dana, J.-Y. Mandin, J. Schroeder, A. McCann, R.R. Gamache, R.B. Watson, K. Yoshino, K.V. Chance, K.W. Jucks, L.R. Brown, V. Nemtchinov, P. Varanasi, J. Quant. Spectrosc. Radiat. Transfer 60 (1998) 665–710.
[11] L.S. Rothman, A. Barbe, D. Chris Benner, L.R. Brown, C. Camy-Peyret, M.R. Carleer, K.V. Chance, K.V. Clerbaux, V. Dana, V.M. Devi, A. Fayt, J.-M. Flaud, R.R. Gamache, A. Goldman, D. Jacquemart, K.W. Jucks, W.J. Lafferty, J.-Y. Mandin, S.T. Massie, D. Newnham, A. Perrin, C.P. Rinsland, J. Schroeder, K. Smith, M.A.H. Smith, R.A. Toth, J. Vander Auwera, P. Prasad, K. Yoshino, J. Quant. Spectrosc. Radiat. Transfer 1–4 (2003) 5–44.
[12] D. Chris Benner, C.P. Rinsland, V. Malathy Devi, M.A.H. Smith, D. Atkins, J. Quant. Spectrosc. Radiat. Transfer 53 (1995) 705–721.
[13] C.R. Pollock, F.R. Peterson, D.A. Jennings, J.S. Wells, A.G. Maki, J. Mol. Spectrosc. 99 (1983) 357–368.
[14] A.D. May, J.D. Poll, Can. J. Phys. 43 (1965) 1836–1842.
[15] A.D. May, V. Degen, J.C. Stryland, H.L. Welsh, Can. J. Phys. 39 (1961) 1769–1783.
[16] A.D. May, G. Varghese, J.C. Stryland, H.L. Welsh, Can. J. Phys. 42 (1964) 1058–1069.
[17] R. Herman, Phys. Rev. 132 (1963) 262–275.
[18] C. Luo, R. Wehr, J.R. Drummond, A.D. May, F. Thibault, J. Boissoles, J.M. Launay, C. Boulet, J.P. Bouanich, J.M. Hartmann, J. Chem. Phys. 115 (2001) 2198–2206.
[19] P.W. Anderson, Phys. Rev. 76 (1949) 647–661.
[20] C.J. Tsao, B. Curnutte, J. Quant. Spectrosc. Radiat. Transfer 2 (1962) 41–91.
[21] A. Predoi-Cross, C. Luo, P.M. Sinclair, A.D. May, J.R. Drummond, J. Mol. Spectrosc. 198 (1999) 291–303.
[22] K. Sung, P. Varanasi, J. Quant. Spectrosc. Radiat. Transfer 83 (2004) 445–458.